REMOTE RAMAN SPECTROSCOPY OF VARIOUS MIXED AND COMPOSITE MINERAL PHASES AT 7.2 m DISTANCE, S. K. Sharma[1], A. K. Misra[1], Syed Ismail[2] and U. N. Singh[2], [1]Hawaii Institute of Geophysics and Planetology, University of Hawaii, Honolulu, Hawaii 96822, USA (sksharma@soest.hawaii.edu), [2]NASA Langley Research Center, Hampton, VA-23681, USA

Introduction: Remote-Raman [e.g.,1-5] and micro-Raman spectroscopy [e.g., 6-10] are being evaluated on geological samples for their potential applications on Mars rover or lander. The Raman lines of minerals are sharp and distinct. The Raman fingerprints of minerals do not shift appreciably but remain distinct even in sub-micron grains and, therefore, can be used for mineral identification in fine-grained rocks [e.g., 4,7]. In this work we have evaluated the capability of a directly coupled remote Raman system (coaxial configuration) for distinguishing the mineralogy of multiple crystals in the exciting laser beam. We have measured the Raman spectra of minerals in the near vicinity of each other and excited with a laser beam (e.g. α-quartz (Qz) and K-feldspar (Feld) plates, each 5 mm thick). The spectra of composite transparent mineral plates of 5 mm thickness of α-quartz and gypsum over calcite crystal were measured with the composite samples perpendicular to the exciting laser beam. The measurements of remote Raman spectra of various bulk minerals, and mixed and composite minerals with our portable UH remote Raman system were carried out at the Langley Research Center in a fully illuminated laboratory.

Experimental Set-up and Samples: The pulsed remote Raman system has been described in detail elsewhere [1-3]. In brief, it consists of a Kaiser F/1.8 Holospec spectrometer equipped with a gated thermoelectrically cooled CCD detector from Princeton Instruments (Model I-MAX-1024-E). A 127-mm telescope (Meade ETX-125 Maksutov Cassegrain, 1900 mm focal length), a frequency-doubled small Nd:YAG pulsed laser source (Model Ultra CFR, Big Sky Laser, 532 nm, 35 mJ/pulse, 20 Hz, pulse width 8 ns, central laser spot divergence 0.5 mrad), The telescope is directly coupled to the spectrometer through a 20x (NA = 0.35, long focal length = 20 mm) microscope lens. A 532 nm SuperNotch Plus holographic filter is used in front of the microscope lens to minimize the Rayleigh scattering signal. The laser beam is made coaxial with the telescope optical axis using two small prisms [2, 11]. All Raman spectra were measured in a coaxial mode with 100 micron slit and the intensified CCD operated in the gated mode with gate width of 1.1 μs. The integration time for each of the spectra for mixed mineral phases and composite mineral phases was 1 s and 30 spectra were accumulated, and the individual mineral spectrum was measured with 1 s integration time with 1 accumulation. Neon lines are used in calibrating the spectra and measured remote Raman spectra of benzene and cyclohexane peak positions are within $\pm$ 2 cm^{-1} of standard values.

The rock-forming mineral samples were purchased from Ward's Natural Science Establishment, Inc. The 5 mm thick plates were cut from α-quartz crystal from Hot Spring, Arkansas, orthoclase crystal ($KAlSi_3O_8$) from Gothic, Colorado, and gypsum, variety Satin spar from Highland Arkansas, USA. Calcite crystal and dolomite samples used as a bulk samples in these experiments were from Chihuahua, Mexico.

Results: The remote Raman spectra of α-quartz and feldspar plates both excited by the laser beam are shown in Fig. 1 along with the spectra of α-quartz and K-feldspar measured individually. The Raman lines of α-quartz and K-feldspar are marked on the mixed Raman spectra by Qz and Feld, respectively.

In the Raman spectra of K-feldspar and α-quartz the strong fingerprint Raman lines of K-feldspar (472 and 512 cm^{-1}) corresponding to symmetric stretching of oxygen of four-membered rings of TO_4 tetrahedra, where T= Si, Al, ν_s(T-O-T) and of α-quartz (462 cm^{-1}) corresponding to symmetric stretching of oxygen of six-membered SiO_4 tetrahedra, ν_s(Si-O-Si) [13-14], are well resolved (Fig. 1). In the mixed spectrum of α-quartz and K-feldspar crystals, the 512 cm^{-1} line of Feld is clearly visible but the 472 cm^{-1} line of Feld overlaps with the strong Qz line at 462 cm^{-1} (Fig. 1 top curve). In addition, the medium intensity lattice modes of Feld at 160 and 281 cm^{-1}, and of Qz at 206 cm^{-1}, along with several weak lines of Feld and Qz are visible in the spectrum of these two minerals excited with the laser beam.

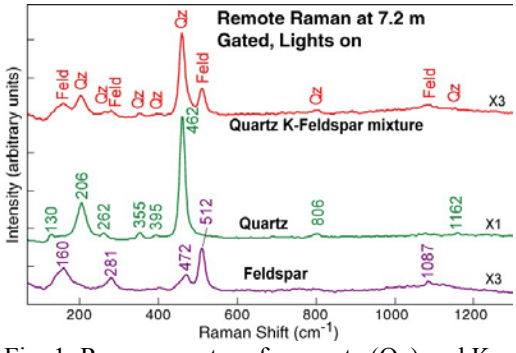

Fig. 1. Raman spectra of α-quartz (Qz) and K-feldspar (Feld) plates side by side illuminated by the laser beam. Individual spectra of α-quartz and K- feldspar are also shown for comparison.

Raman spectra of a composite α-quartz plate over dolomite sample, and of the α-quartz plate and of dolomite minerals are illustrated in Fig. 2. The Raman lines are marked for α-quartz by Qz and those of dolomite by Dol in the composite spectrum of these minerals (top curve in Fig. 2)

In the composite spectrum of α-quartz and dolomite (Fig. 2), the strong fingerprint lines of α-quartz at 462 cm^{-1} corresponding to ν_s(Si-O-Si) mode, and of dolomite at 1099 cm^{-1} corresponding to symmetric stretching mode of oxygen of carbonate ions, $\nu_s(CO_3^{2-})$, are clearly visible. These data indicate that minerals underlying the transparent mineral phase can be detected by remote Raman spectroscopy. The low-frequency lattice modes of medium intensities of dolomite at 176 and 300 cm^{-1}, and of quartz at 206 cm^{-1} are clearly visible in the Raman spectrum of these composite minerals, along with a number of weak bands of α-quartz and dolomite (see top curve in Fig 2).

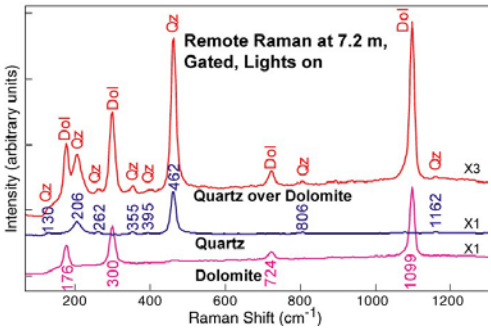

Fig. 2. Remote Raman spectra of a composite α-quartz plate over dolomite mineral (top curve), and of an α-quartz plate, and of a bulk dolomite mineral

Figure 3 shows the Raman spectra of three composite minerals consisting of 5 mm thick plate of α-quartz followed by the 5 mm thick plate of gypsum over a bulk sample of calcite crystal. The 532 nm laser excitation beam first fell on the quartz plate, passed through it and than passed through the gypsum plate and then excited the calcite sample. The Raman lines of α-quartz are marked by Qz, those of gypsum by Gyp, and the Raman lines of calcite by Cal in the composite spectrum of these minerals (top curve in Fig. 3)

In the composite Raman spectrum of α-quartz + gypsum + calcite crystal (Fig. 3, top curve), the strong fingerprints of α-quartz at 462 cm^{-1}, of gypsum at 1006 cm^{-1} corresponding to the symmetric stretch of oxygen of sulfate ions, $\nu_s(SO_4^{2-})$, and the calcite line at 1085 cm^{-1} corresponding to $\nu_s(CO_3^{2-})$ ions of calcite are clearly visible. In addition, the medium intensity lattice modes of quartz and calcite are also detected in the Raman spectra of these composite minerals as marked on the spectrum (Fig. 3). Evidently, the underlying gypsum and calcite minerals can be detected with remote Raman spectroscopy.

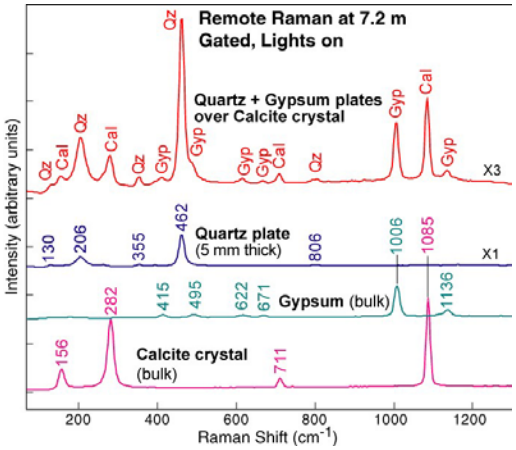

Fig. 3. Raman spectra of three composite minerals: α-quartz and gypsum plates over calcite crystal (top curve); and of α-quartz plate, bulk gypsum and calcite crystals.

Summary: The remote Raman spectra of mixed and composite minerals show the ability of a portable remote Raman system to detect mixed mineral phases and the minerals underlying the transparent minerals from a distance of 7.2 m in a well illuminated background. Such a remote Raman system would be ideal for identifying minerals on a planetary surface during daylight and night time.

Acknowledgments: This work has been supported in part by NASA under a PIDDP grant NAG 5-1301. Two of us (SKS & AKS) gratefully acknowledge travel support provided by the NASA Langley Research Center during the course of this work.

References: [1] Lucey, P.G., et al. (1998) *LPSC XXIX*, Abstract #1354. [2] Sharma, S.K. *et al.* (2002) *Appl. Spectrosc., 56*, 699-705. [3] Sharma, S.K. et al. (2003) *Spectrochim. Acta* A, 59, 2391-2407. [4] Stoper et al. (2004) *Proc. SPIE, 5163*, 99-110 [5] Misra, A.K., et al. [2005] *Spectrochimica Acta A*, *61,* 2281-2287. [6] Haskin L.A., et al. (1997) *JGR 102,* 19,293–19,306. [7] Wang A., et al. (1994) Appl. Spectrosc. 48, 959–968. [8] Wang A. et al. (1999) *JGR 104*, 27,067–27,077. [9] Cooney, T.F., et al. (1999) *Amer. Mineral.,* 84, 1569-1576. [10] Wang A., et al. (1999) *JGR 104*, 8509–8519. [11] Sharma S. K., et al. (2004), *Proc. SPIE, 5660*, 128-138. [12] . [13] Sharma, S.K., et al. (1983) *Amer. Mineral. ,68* (1983) 1113-1125. [14] Matson, D.W., et al. (1986) *Amer. Mineral., 71*, 694-704.